Biochimica et Biophysica Acta 1827 (2013) 387–394

Contents lists available at SciVerse ScienceDirect

Biochimica et Biophysica Acta

journal homepage: www.elsevier.com/locate/bbabio

Formation of an unusually short hydrogen bond in photoactive yellow protein

Keisuke Saito, Hiroshi Ishikita *

202 Building E, Career-Path Promotion Unit for Young Life Scientists, Graduate School of Medicine, Kyoto University, Yoshida-Konoe-cho, Sakyo-ku, Kyoto 606-8501, Japan
Japan Science and Technology Agency (JST), PRESTO, 4-1-8 Honcho Kawaguchi, Saitama 332-0012, Japan

ARTICLE INFO

Article history:
Received 28 July 2012
Received in revised form 12 November 2012
Accepted 16 November 2012
Available online 29 November 2012

Keywords:
Low-barrier hydrogen bond
Proton transfer
Photoactive yellow protein
Laue diffraction crystallography
^{1}H NMR

ABSTRACT

The photoactive chromophore of photoactive yellow protein (PYP) is *p*-coumaric acid (*p*CA). In the ground state, the *p*CA chromophore exists as a phenolate anion, which is H-bonded by protonated Glu46 (O_{Glu46}–O_{pCA} = ~2.6 Å) and protonated Tyr42. On the other hand, the O_{Glu46}–O_{pCA} H-bond was unusually short (O_{Glu46}–O_{pCA} = 2.47 Å) in the intermediate pR_{CW} state observed in time-resolved Laue diffraction studies. To understand how the existence of the unusually short H-bond is energetically possible, we analyzed the H-bond energetics adopting a quantum mechanical/molecular mechanical (QM/MM) approach based on the atomic coordinates of the PYP crystal structures. In QM/MM calculations, the O_{Glu46}–O_{pCA} bond is 2.60 Å in the ground state, where Tyr42 donates an H-bond to *p*CA. In contrast, when the hydroxyl group of Tyr42 is flipped away from *p*CA, the H-bond was significantly shortened to 2.49 Å in the ground state. The same H-bond pattern reproduced the unusually short H-bond in the pR_{CW} structure (O_{Glu46}–O_{pCA} = 2.49 Å). Intriguingly, the potential-energy profile resembles that of a single-well H-bond, suggesting that the pK_a values of the donor (Glu46) and acceptor (*p*CA) moieties are nearly equal. The present results indicate that the "equal pK_a" requirement for formation of single-well or low-barrier H-bond (LBHB) is satisfied only when Tyr42 does not donate an H-bond to *p*CA, and argue against the possibility that the O_{Glu46}–O_{pCA} bond is an LBHB in the ground state, where Tyr42 donates an H-bond to *p*CA.

1. Introduction

Photoactive yellow protein (PYP) serves as a bacterial photoreceptor, in particular, as a sensor for negative phototaxis to blue light [1]. The photoactive chromophore of PYP is *p*-coumaric acid (*p*CA), which is covalently attached to Cys69 [2]. In the PYP ground state, the *p*CA chromophore exists as a phenolate anion [3–5]. The PYP crystal structure revealed that *p*CA is H-bonded by protonated Tyr42 and protonated Glu46 (Fig. 1). Tyr42 is further H-bonded by Thr50. Structural analysis suggested that Glu46 is protonated and *p*CA is ionized in the PYP ground state, pG [6,7]. H atom positions of PYP were assigned in neutron diffraction analysis [8]. According to neutron diffraction analysis, in the case of the Glu46–*p*CA pair, an H atom was at a distance of 1.21 Å from Glu46 and 1.37 Å from *p*CA, almost at the midpoint of the O_{Glu46}–O_{pCA} bond (2.57 Å) (Fig. 1). From this unusual H atom position, the H-bond between Glu46 and *p*CA was interpreted as a low-barrier H-bond [8].

A low-barrier hydrogen bond (LBHB) is a non-standard H-bond, which was originally proposed to possess covalent bond-like characteristics, thus significantly stabilizing the transition state and facilitating enzymatic reactions [9,10]. In original reports by Frey et al. [10] and Cleland and Kreevoy [9], it was stated that an LBHB (including a single-well H-bond) can form when the pK_a difference between donor and acceptor moieties is nearly zero (Fig. 1). If this is the case, the identification of an LBHB can be valid only if the minimum is at the center of the O_{Glu46}–O_{pCA} bond (i.e., the pK_a values of the two moieties are nearly equal) as suggested by Schutz and Warshel [11]. It has been suggested that a stronger H-bond results in a more downfield ^{1}H NMR chemical shift. According to the classification of H-bonds by Jeffrey [12] and Frey [13], "single-well H-bonds" are very short, typically with O–O distances of 2.4 to 2.5 Å, and display ^{1}H NMR chemical shifts (δ_H) of 20 to 22 ppm [13]. "LBHBs" are longer, 2.5 to 2.6 Å, with a δ_H of 17 to 19 ppm [13]. "Weak H-bonds" are even longer, with a δ_H of 10 to 12 ppm [13].

Upon exposure to blue light, PYP undergoes the following photocycle; pG (ground state) → P* –(*trans-cis* isomerization) → I_0 → $I_0^{\ddagger}$ → pR –(proton transfer and large conformational change) → pB → pG [14–16]. The pR to pB transition has been suggested to involve protonation of *p*CA (i.e., proton transfer) and a large structural change of the protein [14,15]. Although time-resolved Laue diffraction studies proposed structural models of the intermediates [17], the relevance of the proposed pB structure (PDB ID: 1TS0) as an intermediate of the photocycle is a matter of debate. In Laue diffraction studies, the pB intermediate has an H-bond between Arg52 and *p*CA [17], whereas solution structures of the pB state argue a high degree of disorder in residues 42–56 [18] (discussed in Ref. [19]).

On the other hand, time-resolved Laue diffraction studies identified the pR_{CW} intermediate [17]. The pR_{CW} intermediate structure [17]

Abbreviations: δ_H, ^{1}H NMR chemical shift; FTIR spectroscopy, Fourier transform infrared spectroscopy; LBHB, low-barrier hydrogen bond; *p*CA, *p*-coumaric acid; PYP, photoactive yellow protein; QM/MM, quantum mechanical/molecular mechanical

* Corresponding author at: 202 Building E, Career-Path Promotion Unit for Young Life Scientists, Graduate School of Medicine, Kyoto University, Yoshida-Konoe-cho, Sakyo-ku, Kyoto 606-8501, Japan. Tel.: +81 75 753 9286; fax: +81 75 753 9281.
E-mail address: hiro@cp.kyoto-u.ac.jp (H. Ishikita).

0005-2728/$ – see front matter © 2012 Elsevier B.V. All rights reserved.
http://dx.doi.org/10.1016/j.bbabio.2012.11.009

was proposed to correspond to the pR species [14–16] observed in spectroscopic studies. The pR state decays to the pB state as a result of PT from Glu46 to *p*CA with the rate coefficient of 250 μs [14,15], which is consistent with that of 333 μs for the pR_{CW} decay [17]. To the best of our knowledge solution structures of the pR state have not been reported.

Interestingly, the O_{Glu46}–O_{pCA} bond is unusually short, 2.47 Å in the pR_{CW} structure (1.60-Å resolution) [17], which may argue against the presence of an LBHB in the ground state proposed in Ref. [8]. In general, an H-bond donor–acceptor distance can be the shortest when the pK_a difference between donor and acceptor moieties is nearly zero. This is why LBHB and single-well H-bonds are shorter than standard (asymmetric double-well) H-bonds (Fig. 1) [11,20–22]. If the presence of the shorter O_{Glu46}–O_{pCA} bond in the pR_{CW} state relative to the ground state is plausible, this will suggest that "matching pK_a" between the H-bond donor and acceptor moieties is not satisfied in the ground state (at least, less likely than in the pR_{CW} state).

The LBHB O_{Glu46}–O_{pCA} bond was originally proposed to stabilize "the isolated negative charge" originating from ionized *p*CA in the protein inner core [8]. However, the presence of the polar residue Tyr42 that donates an H-bond to *p*CA (O_{Tyr42}–O_{pCA} = 2.50 Å [23] to 2.52 Å [8]) in the ground state appeared to play a role in stabilizing the ionized chromophore (Fig. 1) and is possibly an implication that the O_{Glu46}–O_{pCA} bond does not necessarily require characteristics of an LBHB to exist in the protein environment. To understand energetics of the unusually short O_{Glu46}–O_{pCA} bond in the pR_{CW} structure, the influence of Tyr42 (i.e., another H-bond partner of *p*CA) on the O_{Glu46}–O_{pCA} H-bond is to be clarified. In the pR state, the presence of the O_{Glu46}–O_{pCA} H-bond has been confirmed in spectroscopic studies (e.g., the O_{Glu46}–O_{pCA} H-bond is stronger in pR relative to pG [4]), while the presence of the O_{Tyr42}–O_{pCA} is unclear. If the O_{Tyr42}–O_{pCA} H-bond is absent in the pR_{CW} state, pK_a(*p*CA) relative to pK_a(Glu46) is expected to be significantly different from that in the ground state, which can affect the O_{Glu46}–O_{pCA} bond length. Indeed, the O_{Glu46}–O_{pCA} bond is significantly short (2.51 Å) in the Y42F crystal structure [24] relative to the native PYP (2.57 Å [8,23]). Fourier transform infrared (FTIR) spectroscopic studies also have suggested that the O_{Glu46}–O_{pCA} bond is stronger in the Y42F mutant than in the native PYP [25].

To evaluate how formation of an unusually short H-bond is energetically possible in PYP, we analyzed the H-bond energetics adopting a quantum mechanical/molecular mechanical (QM/MM) approach based on the atomic coordinates of the PYP crystal structures including the pR_{CW} [17] and Y42F [24] structures.

2. Computational procedures

2.1. QM/MM calculations

The atomic coordinates were taken from the X-ray structures of the native (PDB ID: 1OT9 or 1OTB) [23] and Y42F (1F9I) [24], PYP proteins and the Laue crystal structure of the pR_{CW} (1TS7) intermediate [17]. To gain better understanding of the electronic structure of the chromophore *p*CA, and the residues in the H-bond network, namely Tyr42, Glu46, Thr50, and Cys69, we performed large-scale QM/MM calculations for the entire PYP protein. Note that the calculated O_{Glu46}–O_{pCA} H-bond length remained unchanged even when Cys69 was involved in the MM region. We employed the so-called electrostatic embedding QM/MM scheme [26] and used the Qsite [27] program code as performed in previous studies [28]. The detailed geometry of QM region was optimized under the influence of MM electrostatic/steric field (see PYP_SI.pdb in SI for geometry). We employed the restricted DFT method with the B3LYP functional and LACVP**+ basis sets. Forthe QM/MM calculations, we added additional counter ions to neutralize the whole system.

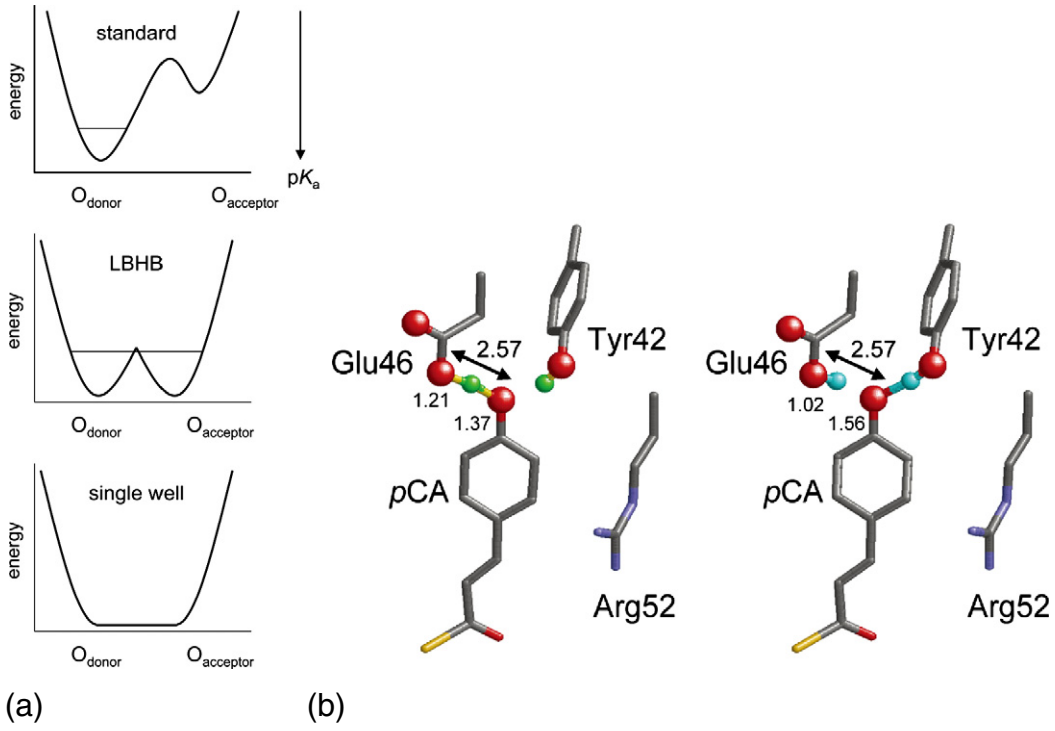

Fig. 1. (a) Overview of typical potential-energy profiles: (top) standard H-bonds (asymmetric double-well), typically with an O_{donor}–$O_{acceptor}$ distance > ~2.6 Å; (middle) low barrier H-bond (LBHB), typically with an O_{donor}–$O_{acceptor}$ distance of 2.5–2.6 Å; and (bottom) single-well (ionic) H-bonds, typically with an O_{donor}–$O_{acceptor}$ distance of < ~2.5 Å [20]. (b) H atom positions of the O_{Glu46}–O_{pCA} bond (left) in the neutron diffraction analysis (green sphere, PDB ID: 2ZOI) [8]. (right) QM/MM optimized structure based on the X-ray crystal structure (cyan sphere, PDB ID: 1OT9) [23].

2.2. H-bond potential-energy

For following the proton transfer (PT) pathways, we employed an iterative (constrained) QM/MM geometry optimizations with fixing the selected reaction coordinate. First, we prepared for the QM/MM optimized geometry without constraints, and we used the resulting geometry as the initial geometry. Next, the reaction coordinate was defined as a linear combination of two PT distances (O_{donor}–H and H–$O_{acceptor}$). Then, we moved the H atom from the H-bond donor atom (O_{donor}) to the acceptor atom ($O_{acceptor}$) by 0.05 Å, optimized the geometry by constraining the O_{donor}–H and H–$O_{acceptor}$ distances such that the sum of the two distances remained constant in order to really follow the proton motion, and calculated the energy of the resulting geometry at each PT coordinate. This procedure was repeated until the H atom reached the $O_{acceptor}$ atom. Except for the atoms directly involved in the PT reaction coordinate (i.e., O_{donor}, a transferring H, and $O_{acceptor}$ atoms), all of the atomic coordinates in the QM region were fully relaxed (i.e., not fixed) in the generation of the scans.

2.3. ^{1}H NMR chemical shift

The NMR chemical shift was calculated by using the GIAOs method [29] implemented in the Qsite [27] and JAGUAR [30] programs. The absolute shielding constant of ^{1}H of tetramethylsilane (TMS) was calculated to be 31.6 ppm on the basis of the atomic coordinates in Ref. [31] and used as the TMS reference for δ_H. We evaluated the accuracy of the quantum chemically calculated δ_H [32]. First, we calculated δ_H for maleate and compounds which are also supposed to contain a strong H-bond or an LBHB [33]. The calculated δ_H values are considerably close to the experimentally measured values, with discrepancies of ~1 ppm or less [32]. The discrepancy between the measured values (solution) and the calculated values (solid state) is mainly due to inadequate accounting for the multiconfiguration of the molecular geometry, the proton dynamics, and the rovibrational corrections to the nuclear shielding in the calculations. This indicates, however, that the contributions of these features to the values are obviously negligible, which does not practically affect any conclusions from the present study. Hence, the calculated δ_H values should be considered at this level of accuracy [32].

2.4. ^{1}H NMR chemical shift validation

The calculated OHO-bond geometries and the NMR chemical shifts can also be evaluated by the correlation proposed by Limbach et al. [34]. The geometric correlation of the $O_{acceptor}$···H–O_{donor} bond between the acceptor···hydrogen ($O_{acceptor}$···H) distance r_1 and the donor–hydrogen (O_{donor}–H) distance r_2 can be obtained by

$$\begin{aligned} q_2 &= 2r^0 + 2q_1 + 2b\ \ln[1 + \exp(-2q_1/b)],\\ b &= \left[2\ q_{2\min} - 2\ r^0\right]/(2\ \ln 2),\\ q_1 &= (r_1 - r_2)/2,\\ q_2 &= r_1 + r_2, \end{aligned} \tag{1}$$

where q_{2min} represents a minimum value corresponding to the minimum $O_{acceptor}$···O_{donor} distance in the case of a linear H-bond, and r^0 is the equilibrium distance in the fictive free diatomic unit OH [34]. The correlation between the OHO-bond geometry and the ^{1}H NMR chemical shift δ_H can be obtained by

$$\begin{aligned} \delta_H &= {\delta_{OH}}^0 + \Delta_H(4p_1p_2)^m,\\ p_1 &= \exp\left[-\left(q_1 + q_2/2 - r^0\right)/b\right],\\ p_2 &= \exp\left[-\left(-q_1 + q_2/2 - r^0\right)/b\right], \end{aligned} \tag{2}$$

where δ^0_{OH} and Δ_H represent the limiting chemical shifts of the separate fictive groups OH and the excess chemical shift of the quasi-symmetric complex, respectively, and m is an empirical parameter. q_2 is given in Eq. (1). Using Eqs. (1) and (2), the δ_H can also be obtained, regarding q_2 as the donor–acceptor (O_{donor}–$O_{acceptor}$) distance. We used the same parameters as used in Ref. [34], i.e., $r^0 = 0.93$, $q_{2min} = 2.36$, $\delta^0_{OH} = 7.9$, $\Delta_H = 13$, and $m = 1.1$, as done in a previous study [32].

3. Results

3.1. Influence of Tyr42 on the O_{Glu46}–O_{pCA} bond properties

In the QM/MM geometry, the O_{Glu46}–O_{pCA} bond of 2.51 Å in the Y42F mutant is shorter than the bond of 2.57 Å in the native PYP, in agreement with the crystal structure [24] (Table 1). The calculated δ_H value for the O_{Glu46}–O_{pCA} bond in the Y42F mutant was 16.8 ppm (Table 1), in agreement with a δ_H of 16.7 ppm measured in solution NMR studies [35]. Using the correlation proposed by Limbach et al. (Eqs. 1 and 2) [34], an O–O distance of 2.51 Å also predicts a δ_H of 16.4 ppm, suggesting that the larger δ_H in the Y42F mutant is predominantly due to the decreased O_{Glu46}–O_{pCA} length.

The decrease in the O_{Glu46}–O_{pCA} length upon mutation of Y42F can also be understood from the decrease in the energy near the *p*CA moiety relative to the Glu46 moiety in the potential energy profile (Fig. 3), which corresponds to the decrease in the pK_a difference between Glu46 and *p*CA. Thus, the shorter O_{Glu46}–O_{pCA} length in the Y42F mutant with respect to the native PYP is due to pronounced "matching pK_a" between the H-bond donor and acceptor moieties, i.e. the H-bond potential energy shape becomes more symmetric. Similar relationship between the pK_a differences and the H-bond donor–acceptor distances has also been demonstrated for H-bonds in other proteins (e.g., counter ions in bacteriorhodopsin and *Anabaena* sensory rhodopsin [36] and redox active tyrosine D1-Tyr161 in photosystem II [37]).

Such a decrease in the pK_a difference leads to a more symmetrical H bond characteristic of the O_{Glu46}–O_{pCA} bond. According to Frey [13], an essential requirement for a symmetrical H-bond is that the proton lies inline with the donor and acceptor atoms; this feature is pronounced in the essentially linear H-bond of O_{Glu46}–H–O_{pCA} in the Y42F mutant (172.0°) relative to the that in the native PYP (168.2°)

Table 1
(i) Experimental and calculated geometries (in Angstrom for distance and degree for angle) and (ii) δ_H (in ppm) of the mutant PYP proteins. For the complete atomic coordinates of the QM/MM geometries, see PYP_SI.pdb in SI. n.d.; not determined.

(i)

	Native		Y42F	
	Crystal		Crystal	
	(1OT9)	Calc.	(1F9I)	Calc.
O_{Glu46}–O_{pCA}	2.59	2.57	2.51	2.50
O_{Glu46}–H	n.d.	1.02	n.d.	1.04
H–O_{pCA}	n.d.	1.56	n.d.	1.47
(O_{Glu46}–H–O_{pCA})	n.d.	168.2	n.d.	172.0
O_{Tyr42}–O_{pCA}	2.50	2.48	n.d.	n.d.
O_{Tyr42}–H	n.d.	1.02	n.d.	n.d.
H–O_{pCA}	n.d.	1.47	n.d.	n.d.
(O_{Tyr42}–H–O_{pCA})	n.d.	170.9	n.d.	n.d.
O_{Thr50}–O_{Tyr42}	2.85	2.79	n.d.	n.d.
O_{Thr50}–$O_{C=O,\ 46}$	3.13	3.08	3.23	3.22
O_{Thr50}–O_{pCA}	4.02	4.01	2.79	2.76

(ii)

	Native		Y42F	
	Solution	Calc.	Solution	Calc.
Glu46	15.2[a]	14.8	16.7[a]	16.8
Tyr42	13.7[a]	14.9	n.d.	n.d.

[a] See Ref. [35].

Table 2
(i) Experimental and calculated geometries (in Angstrom for distance and degree for angle) and (ii) δ_H (in ppm) of the native PYP. For the complete atomic coordinates of the QM/MM geometries, see PYP_SI.pdb in SI. n.d.; not determined. The error in O–O distance in the crystal was estimated to be 0.01–0.02 Å [23].

(i)

	Native		
	1OT9	Calc.	Calc.
[Geometry]		Standard	Short O_{Glu46}–O_{pCA}
O_{Glu46}–O_{pCA}	2.59	2.57	2.46
O_{Glu46}–H	n.d.	1.02	1.07
H–O_{pCA}	n.d.	1.56	1.39
(O_{Glu46}–H–O_{pCA})	n.d.	168.2	169.9
O_{Tyr42}–O_{pCA}	2.50	2.48	2.70
O_{Tyr42}–H	n.d.	1.02	0.97
H–O_{pCA}	n.d.	1.47	3.20
(O_{Tyr42}–H–O_{pCA})	n.d.	170.9	51.1
O_{Thr50}–O_{Tyr42}	2.85	2.79	2.86
O_{Thr50}–$O_{C=O,\ 46}$	3.13	3.08	2.81
O_{Thr50}–O_{pCA}	4.02	4.01	4.09

(ii)

		Standard	Short O_{Glu46}–O_{pCA}
	Solution	Calc.	Calc.
Glu46	15.2[a]	14.8	18.8
Tyr42	13.7[a]	14.9	5.7

[a] See Ref. [35].

(Table 1). All these features are consistent with previous proposals by Frey et al. [10,13], Cleland and Kreevoy [9], Schutz and Warshel [11], and Limbach et al. [34]. Note that the resulting properties of the potential-energy curve and δ_H calculated for the present crystal structure of the native PYP (PDB ID: 1OT9, 110K) are consistent with those previously reported for the other crystal structure (PDB ID: 2ZOH, 295K) [28,32].

In summarizing the results, the H-bond donation of Tyr42 to *p*CA contributes to the increase in the O_{Glu46}–O_{pCA} length of the native PYP (2.57 Å) relative to the Y42F mutant (2.51 Å).

3.2. Influence of Tyr42 on the O_{Glu46}–O_{pCA} length in the native PYP

In contrast to the Y42F mutant, it is obvious that Tyr42 donates an H-bond to *p*CA in the ground state of the native PYP [8,28,32]. To investigate the influence of Tyr42 as an H-bond donor to *p*CA on the H-bond network, we performed QM/MM calculations by flipping the hydroxyl group of Tyr42 (i.e., without removing Tyr42). Note that Thr50 is at an H-bond distance with Tyr42 (2.85 Å) in the crystal structure [23] (Table 2).

We found that, if Tyr42 provides an H-bond to Thr50, not to *p*CA, the H-bond geometry resulted in an unusually short O_{Glu46}–O_{pCA} bond of 2.46 Å ([short O_{Glu46}–O_{pCA}] bond pattern, Fig. 2) with a δ_H of 18.8 ppm, typical values for symmetrical H-bonds [13] (Table 2). The potential-energy curve of [short O_{Glu46}–O_{pCA}] resembles that of a single-well H-bond as shown in Ref. [20] (Fig. 4). The number of H

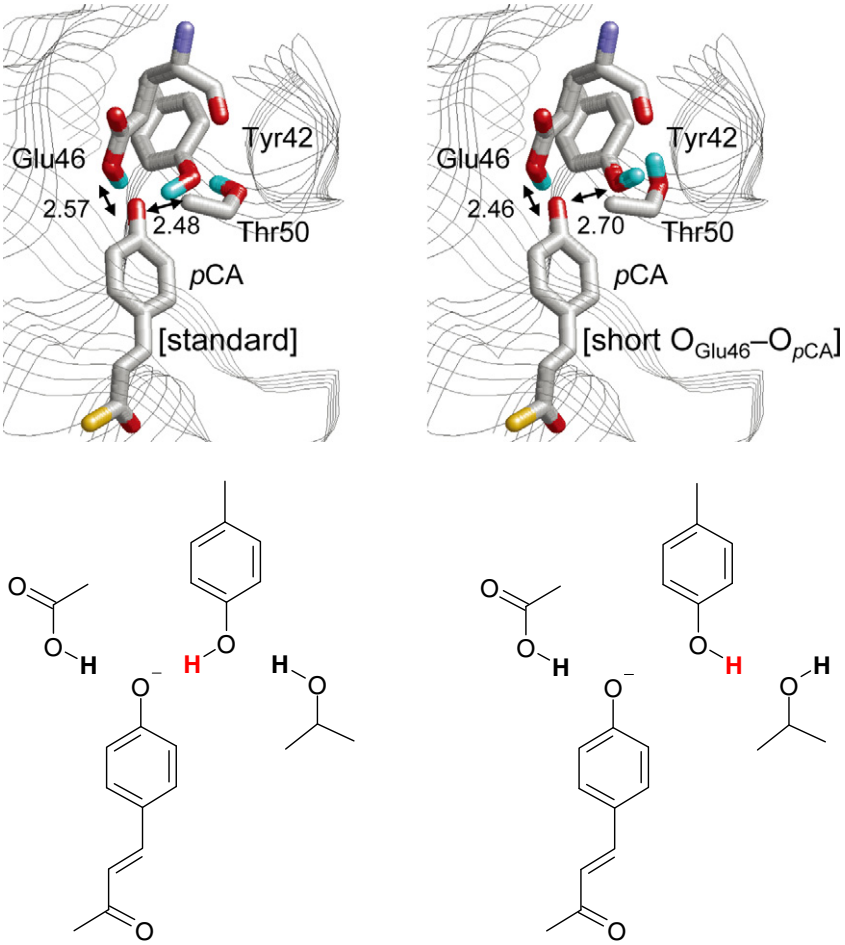

Fig. 2. Possible H-bond patterns in the native PYP. QM/MM optimized geometries of (left) the [standard] and (right) [short O_{Glu46}–O_{pCA}] H-bond patterns.

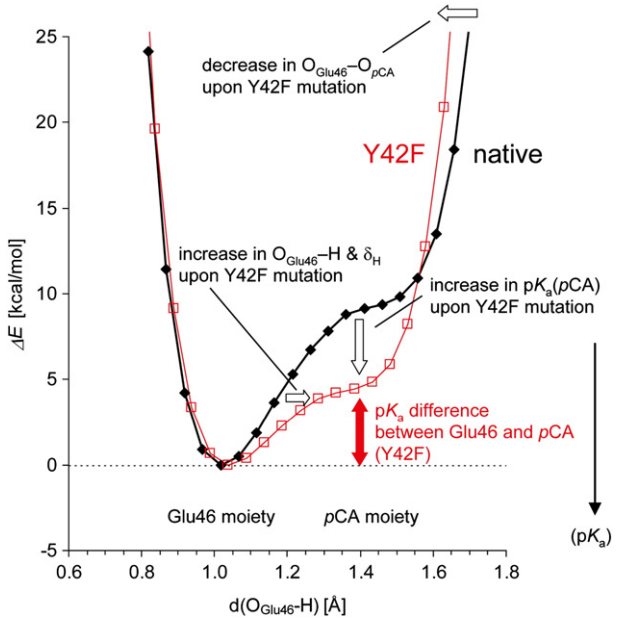

Fig. 3. Energy profiles along the proton transfer coordinate for the O_{Glu46}–O_{pCA} bond in the native PYP (black curve) and the Y42F mutant (red curve). Changes of the properties induced by the Y42F mutation are indicated by open arrows. For comparison, the energy minimum was set to zero for both the native PYP and the Y42F mutant. Although pK_a should refer to free energy rather than energy, it can be practically assumed to result in the same tendency [40], in particular for the case with short H-bonds where the proton motion is considerably restricted due to the presence of the donor and acceptor moieties in the protein environment. Note that pK_a is not for a proton release from the O_{donor}–H…$O_{acceptor}$ bond (i.e., pK_a ([O_{donor}–H…$O_{acceptor}$]/[O_{donor}…$O_{acceptor}$]$^-$)), but pK_a ([O_{donor}–H]/[O_{donor}]$^-$) and pK_a ([$O_{acceptor}$–H]/[$O_{acceptor}$]$^-$) for each diabatic potential curve of the donor/acceptor moiety [41].

bonds in the chromophore of the [short O_{Glu46}–O_{pCA}] geometry is identical to the [standard] H-bond geometry where Tyr42 provides an H-bond to *p*CA (Fig. 2). These results demonstrate that Tyr42 in the native PYP is the residue that prevents Glu46 and *p*CA from possessing equal pK_a. A symmetrical H-bond is unlikely to form between Glu46 and *p*CA as long as Tyr42 provides an H-bond to *p*CA.

Notably, the neutron diffraction geometry (in the ground state) confirmed the presence of an H-bond donation from Tyr42 to *p*CA [8], which strongly suggests that in the ground state, O_{Glu46}–O_{pCA} is chemically impossible to form a symmetrical H-bond due to the obvious pK_a difference between Glu46 and *p*CA induced by Tyr42. If formation of an LBHB were strongly advantageous, then the hydrogen bond pattern would rearrange to allow formation of an LBHB in the ground state. Hence, to flip the Tyr42 H-bond and to form a single-well H-bond, a large energy is required (Fig. 4), which may be possible only upon photoexcitation (discussed later).

3.3. Energetics of a single-well H-bond

One might consider that the [short O_{Glu46}–O_{pCA}] bond of 2.46 Å with a δ_H of 18.9 ppm is a strong H-bond. However, the potential-energy curve of the [short O_{Glu46}–O_{pCA}] bond (QM/MM energy, corresponding to represent not only the energy of the QM region but also contain that of the remaining protein environment) was significantly, energetically high relative to that of the [standard O_{Glu46}–O_{pCA}] bond geometry (Fig. 4). The observed chromophore destabilization was mainly due to the loss of O_{Tyr42}–O_{pCA} H-bond. The short O_{Glu46}–O_{pCA} bond of 2.46 Å is ~4 kcal/mol more stabilized than the [standard O_{Glu46}–O_{pCA}] bond of 2.57 Å. However, complete loss of the O_{Tyr42}–O_{pCA} H-bond is much more energetically disadvantageous. In addition, it also induces repulsion between O_{Tyr42} and O_{pCA} (~6 kcal/mol), destabilizing the chromophore region. (Note: That the corresponding repulsion is absent

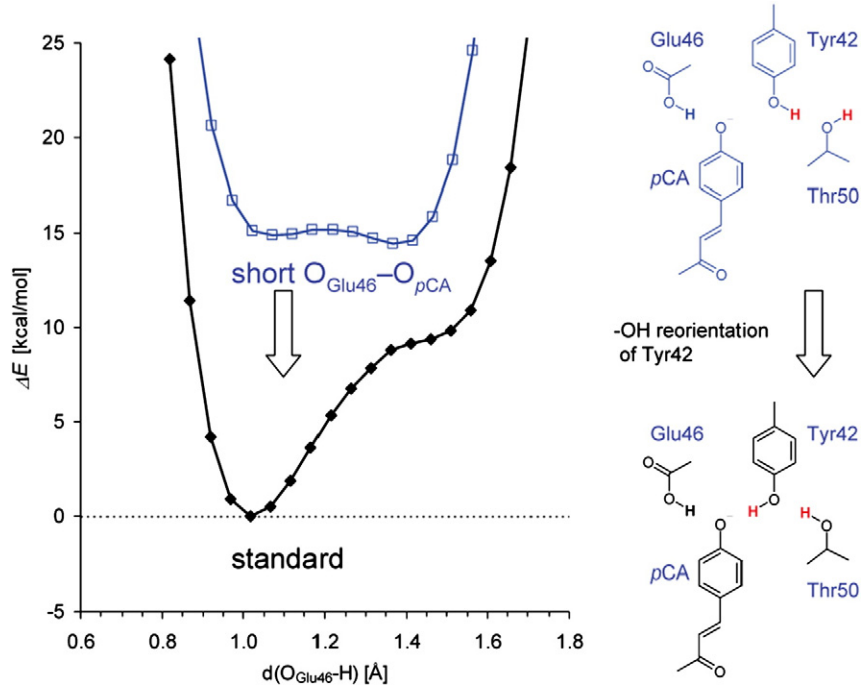

Fig. 4. Energy profiles along the proton transfer coordinate for the O_{Glu46}–O_{pCA} bond in the [standard] H-bond geometry (black curve) and the short O_{Glu46}–O_{pCA} bond geometry (blue) in the native PYP. The two H-bond patterns differ predominantly at the H atom (red) orientation of Tyr42. The open arrows indicate a reorientation of the hydroxyl H atom of Tyr42, which separates the two H-bond geometries energetically. Note that the atomic coordinates of Tyr42 were fully relaxed (not fixed) in each QM/MM calculation. The energy minimum of the [standard] H-bond geometry was set to zero. The two energy profiles describe the total QM/MM energy of the entire system, including both QM and MM regions.

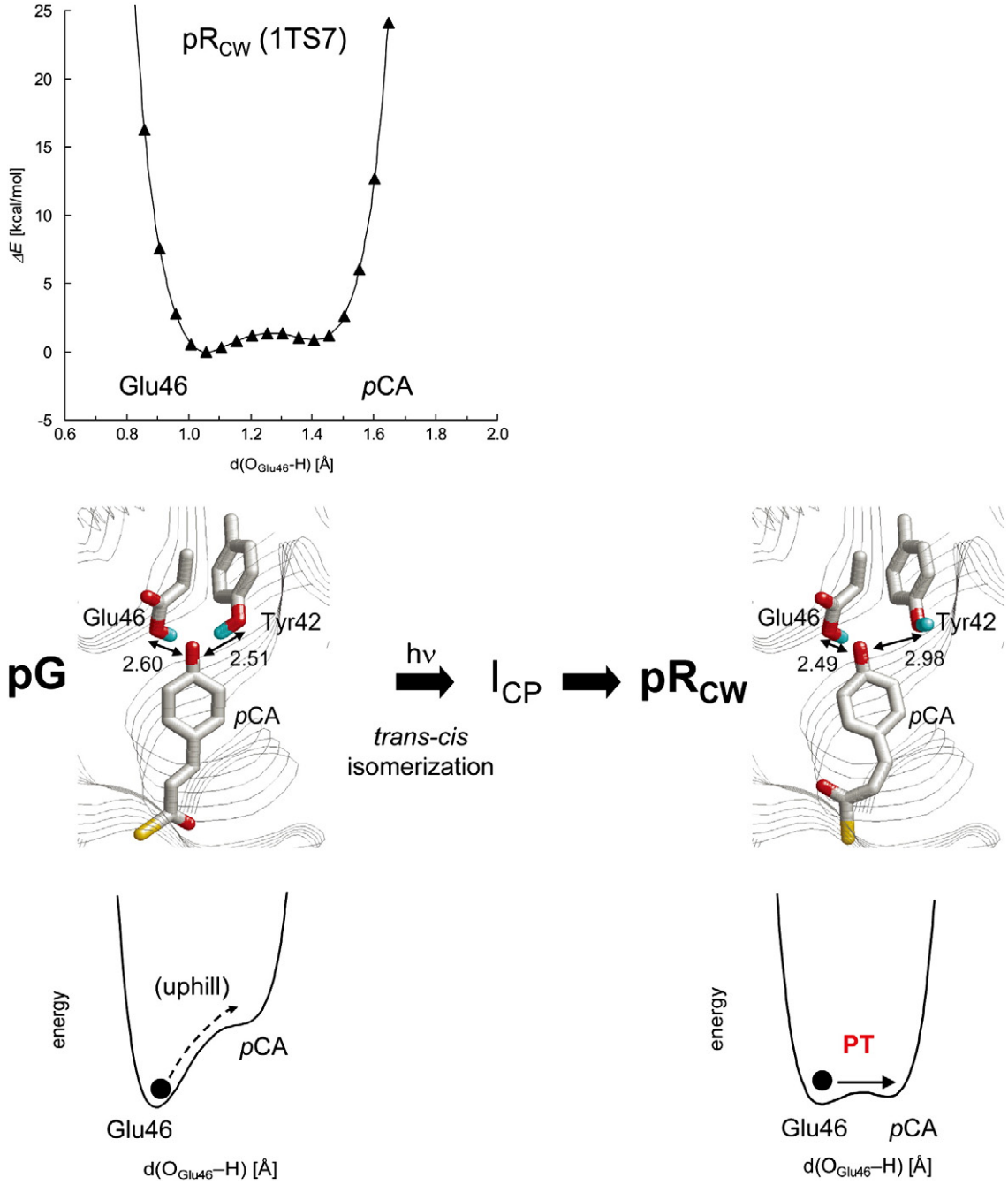

Fig. 5. Energy profiles along the proton transfer coordinate for the O_{Glu46}–O_{pCA} bond in the pR_{CW} intermediate (PDB ID: 1TS7).

in the Y42F mutant due to the absence of O_{Tyr42}. Thus, pK_a (*p*CA) is slightly lower than pK_a (Glu46) in the Y42F mutant (Fig. 3) in contrast to the [short O_{Glu46}–O_{pCA}] geometry (Fig. 4) or the pR_{CW} structure (Fig. 5).)

One advantage of the catalytic site of the protein over bulk water is the availability of the preorganized dipoles in the protein environment to stabilize the transition state electrostatically [11,21]. For enzymes to utilize the protein dipoles effectively in stabilizing the transition state, a larger polarity between the transition state and the protein is energetically advantageous. In the case of PYP, Tyr42 obviously plays a role in providing the corresponding large polarity to the stability of the O_{Glu46}–O_{pCA} bond, which energetically suppresses formation of an LBHB in O_{Glu46}–O_{pCA}. Hence, formation of a short H-bond does not necessarily lower the total energy of the protein, as previously reported in other studies [11,21,22].

3.4. Influence of the H-bond between the carbonyl group of pCA and the backbone amide of Cys69 on the O_{Glu46}–O_{pCA} length

The [short O_{Glu46}–O_{pCA}] geometry and the pR_{CW} structure have the same H-bond patterns of Glu46, *p*CA, and Tyr42, where the O_{Glu46}–O_{pCA} and O_{Tyr42}–O_{pCA} H-bonds are present and absent, respectively (discussed later). On the other hand, the H-bond between the carbonyl group of *p*CA and the amide group of Cys69, is present in the [short O_{Glu46}–O_{pCA}] geometry but absent in the pR_{CW} structure [17]. Irrespective of the difference in the H-bond pattern of Cys69, the O_{Glu46}–O_{pCA} bond lengths are similarly, unusually short in the two structures (Tables 2 and 3). Hence, the presence/absence of the H-bond of Cys69 on the O_{Glu46}–O_{pCA} length appears to be much less crucial to the O_{Glu46}–O_{pCA} bond length than that of Tyr42.

Table 3
Experimental and calculated geometries (in Angstrom for distance and degree for angle) of the pR_{CW} intermediate identified in time-resolved Laue crystallography [17]. Values for the native PYP with the [standard] H-bond pattern are also shown for comparison. For the complete atomic coordinates of the QM/MM geometries, see PYP_SI.pdb in SI. n.d.; not determined.

	Dark		pR_{CW}		
	1OTB	Calc.	1TS7	Calc.	Calc.
[Geometry]		Standard		Short O_{Glu46}–O_{pCA}	Standard
O_{Glu46}–O_{pCA}	2.58	2.60	2.47	2.49	2.60
O_{Glu46}–H	n.d.	1.02	n.d.	1.06	1.02
H–O_{pCA}	n.d.	1.59	n.d.	1.43	1.59
(O_{Glu46}–H–O_{pCA})	n.d.	170.1	n.d.	172.7	171.2
O_{Tyr42}–O_{pCA}	2.51	2.51	2.83	2.98	2.55
O_{Tyr42}–H	n.d.	1.02	n.d.	0.97	1.02
H–O_{pCA}	n.d.	1.50	n.d.	n.d.	1.53
(O_{Tyr42}–H–O_{pCA})	n.d.	170.3	n.d.	n.d.	174.9
O_{Thr50}–O_{Tyr42}	2.89	2.84	2.83	2.83	2.89
O_{Thr50}–$O_{C=O,\ 46}$	3.17[a]	3.05	3.38	2.74	3.24

[a] See Ref. [35].

4. Discussion

4.1. Presence of a single-well H-bond in the pR_{CW} intermediate structure in time-resolved Laue crystallography

The O_{Glu46}–O_{pCA} bond is unusually short, 2.47 Å in the pR_{CW} structure (Table 3). However, the H atom positions and thus far H-bond pattern are yet not known from the crystal structure. The QM/MM calculations reproduced the unusually short H-bond distance (2.49 Å) on the basis of the pR_{CW} structure only when the [short O_{Glu46}–O_{pCA}] H-bond geometry (Fig. 2) was assumed (Table 3). The standard O_{Glu46}–O_{pCA} H-bond geometry (i.e., Tyr42 donates an H-bond to *p*CA) yielded the bond length of 2.60 Å even in QM/MM calculations of the pR_{CW} structure. These results confirm that the actual H-bond pattern in the pR_{CW} crystal structure is the [short O_{Glu46}–O_{pCA}] H-bond geometry, where Tyr42 is flipped away from *p*CA, rather than the [standard O_{Glu46}–O_{pCA}] H-bond geometry, where Tyr donates an H-bond to *p*CA.

The existence of the unusually short H-bond appears to be plausible not only in the pR_{CW} structure [17], but also in the pR species [14–16] observed in spectroscopic studies. FTIR studies have suggested that the H-bond between Glu46 and *p*CA becomes stronger in pR relative to pG as suggested by the downshift in the C=O stretching frequency of protonated Glu46 [4]. Because shortening an H-bond donor and acceptor distance leads to migration of the H atom toward the acceptor moiety (e.g., Ref. [32,36]), the observed downshift in the C=O stretching frequency of Glu46 is consistent with the presence of the unusually short O_{Glu46}–O_{pCA} bond in the pR_{CW} structure. Significance of the H-bond pattern of Tyr42 and *p*CA in the O_{Glu46}–O_{pCA} length can also be seen in studies of the Y42F mutant: (i) the Y42F crystal structure [24] has a shorter O_{Glu46}–O_{pCA} bond than the native PYP (Table 1) and (ii) the C=O stretching frequency of protonated Glu46 in the Y42F mutant is downshifted relative to the wild type PYP in FTIR studies [25].

Interestingly, the potential-energy curve of the O_{Glu46}–O_{pCA} bond (2.49 Å) in the pR_{CW} crystal structure resembles that of a typical single-well H-bond; the barrierless potential for the PT is an indication of the pR_{CW} intermediate being ready for the PT (Fig. 5). In FTIR studies, the C=O stretching frequency for protonated Glu46 is downshifted to 1732 cm^{-1} in pR relative to 1740 cm^{-1} in pG, suggesting that the H atom in the O_{Glu46}–O_{pCA} bond (i) remains in the Glu46 moiety (i.e. can interact with Glu46) but simultaneously (ii) significantly migrated toward the *p*CA moiety [4]; this is exactly the case for a single-well H bond. Indeed, in FTIR studies the existence of a single-well H-bond has been already proposed [4]; a stronger H-bond in pR relative to pG lowers the energy barrier for proton transfer from Glu46 to *p*CA (see also Fig. 4 in Ref. [4]). The present study confirms this, by demonstrating that the unusually short H-bond in the pR_{CW} crystal structure [17] is reproducible on the basis of quantum chemistry.

The O_{Glu46}–O_{pCA} H-bond is absent in the pB state [4] and solution structures of the pB state [18]. If the short O_{Glu46}–O_{pCA} H-bond could be a very strong bond, the pR_{CW} intermediate would be very stable and the proceeding pB state would never form in such a time scale. It should also be noted that a lifetime of hundreds μs for the pR_{CW} state is due to the large structural change rather than the PT from Glu46 to *p*CA. In addition, in a single-well H-bond, movement of a proton between the donor and acceptor moieties is not directly associated with breakage of the H-bond. (Note: The potential energy profile of a single-well H-bond only suggests that movement of a proton is easier than in a standard H-bond due to the absence of the energy barrier.) Breakage of the short O_{Glu46}–O_{pCA} H-bond can occur as a result of the large structural change, which is driven by the photon energy stored in the system [38]. Hence, the pR intermediate can lower the energy to proceed the pB state by abolishing the unusually short O_{Glu46}–O_{pCA} H-bond of <2.5 Å.

Here, one may also rediscover the so-called "principle of frustration", where in the folding process, proteins (may not completely eliminate but at least) need to minimize frustration [39]. In terms of the "local" H-bond network of *p*CA, formation of the unusually short H-bond is energetically allowed (or favored) at the stage of the pR intermediate. However, this is not the energetically lowest state of the "entire" protein, which can also be understood by pR being followed by pB.

5. Concluding remarks

The presence of the shorter O_{Glu46}–O_{pCA} bond (2.47 Å) in the pR_{CW} crystal structure [17] relative to the ground state structure (2.57 Å) indicates that the "equal pK_a" requirement for formation of a single-well H-bond is satisfied in the pR_{CW} intermediate, but not in the ground state. If matching pK_a were satisfied in the ground state, the O_{Glu46}–O_{pCA} bond (~2.6 Å [8,23]) could neither be further shorten to ~2.5 Å in the pR_{CW} structure [17] nor become stronger in pR as observed in FTIR studies [4]. An LBHB or a single-well H-bond is less likely to form between Glu46 and *p*CA as long as Tyr42 provides an H-bond to *p*CA in the native PYP.

The present case clearly shows that the formation of a short symmetrical H-bond does not necessarily help to decrease the total energy of the active site. Comparison of the energetics of the two possible H-bond patterns in the same protein unambiguously enabled us to realize that merely focusing on a short H-bond might lead to neglect of the total energy.

Acknowledgement

This research was supported by the JST PRESTO program (K.S. and H.I), Grant-in-Aid for Scientific Research from the Ministry of Education, Culture, Sports, Science and Technology (MEXT) of Japan (22740276 to K.S.), Special Coordination Fund for Promoting Science and Technology of MEXT (H.I), Takeda Science Foundation (H.I.), Kyoto University Step-up Grant-in-Aid for Young Scientists (H.I.), and Grant for Basic Science Research Projects from The Sumitomo Foundation (H.I.).

Appendix A. Supplementary data

Supplementary data to this article can be found online at http://dx.doi.org/10.1016/j.bbabio.2012.11.009.

References

[1] W.W. Sprenger, W.D. Hoff, J.P. Armitage, K.J. Hellingwerf, The eubacterium *Ectothiorhodospira halophila* is negatively phototactic, with a wavelength dependence that fits the absorption spectrum of the photoactive yellow protein, J. Bacteriol. 175 (1993) 3096–3104.

[2] M. Baca, G.E. Borgstahl, M. Boissinot, P.M. Burke, D.R. Williams, K.A. Slater, E.D. Getzoff, Complete chemical structure of photoactive yellow protein: novel thioester-linked 4-hydroxycinnamyl chromophore and photocycle chemistry, Biochemistry 33 (1994) 14369–14377.

[3] M. Kim, R.A. Mathies, W.D. Hoff, K.J. Hellingwerf, Resonance Raman evidence that the thioester-linked 4-hydroxycinnamyl chromophore of photoactive yellow protein is deprotonated, Biochemistry 34 (1995) 12669–12672.

[4] A. Xie, W.D. Hoff, A.R. Kroon, K.J. Hellingwerf, Glu46 donates a proton to the 4-hydroxycinnamate anion chromophore during the photocycle of photoactive yellow protein, Biochemistry 35 (1996) 14671–14678.

[5] E. Demchuk, U.K. Genick, T.T. Woo, E.D. Getzoff, D. Bashford, Protonation states and pH titration in the photocycle of photoactive yellow protein, Biochemistry 39 (2000) 1100–1113.

[6] G.E. Borgstahl, D.R. Williams, E.D. Getzoff, 1.4 Å structure of photoactive yellow protein, a cytosolic photoreceptor: unusual fold, active site, and chromophore, Biochemistry 34 (1995) 6278–6287.

[7] E.D. Getzoff, K.N. Gutwin, U.K. Genick, Anticipatory active-site motions and chromophore distortion prime photoreceptor PYP for light activation, Nat. Struct. Biol. 10 (2003) 663–668.

[8] S. Yamaguchi, H. Kamikubo, K. Kurihara, R. Kuroki, N. Niimura, N. Shimizu, Y. Yamazaki, M. Kataoka, Low-barrier hydrogen bond in photoactive yellow protein, Proc. Natl. Acad. Sci. U. S. A. 106 (2009) 440–444.

[9] W.W. Cleland, M.M. Kreevoy, Low-barrier hydrogen bonds and enzymic catalysis, Science 264 (1994) 1887–1890.

[10] P.A. Frey, S.A. Whitt, J.B. Tobin, A low-barrier hydrogen bond in the catalytic triad of serine proteases, Science 264 (1994) 1927–1930.

[11] C.N. Schutz, A. Warshel, The low barrier hydrogen bond (LBHB) proposal revisited: the case of the Asp… His pair in serine proteases, Proteins 55 (2004) 711–723.

[12] G.A. Jeffrey, An Introduction to Hydrogen Bonding, Oxford University Press, Oxford, 1997.

[13] P.A. Frey, in: A. Kohen, H.-H. Limbach (Eds.), Isotope Effects in Chemistry and Biology, CRC Press, Boca Raton, FL, 2006, pp. 975–993.

[14] W.D. Hoff, I.H. van Stokkum, H.J. van Ramesdonk, M.E. van Brederode, A.M. Brouwer, J.C. Fitch, T.E. Meyer, R. van Grondelle, K.J. Hellingwerf, Measurement and global analysis of the absorbance changes in the photocycle of the photoactive yellow protein from *Ectothiorhodospira halophila*, Biophys. J. 67 (1994) 1691–1705.

[15] L. Ujj, S. Devanathan, T.E. Meyer, M.A. Cusanovich, G. Tollin, G.H. Atkinson, New photocycle intermediates in the photoactive yellow protein from *Ectothiorhodospira halophila*: picosecond transient absorption spectroscopy, Biophys. J. 75 (1998) 406–412.

[16] M. Unno, M. Kumauchi, N. Hamada, F. Tokunaga, S. Yamauchi, Resonance Raman evidence for two conformations involved in the L intermediate of photoactive yellow protein, J. Biol. Chem. 279 (2004) 23855–23858.

[17] H. Ihee, S. Rajagopal, V. Srajer, R. Pahl, S. Anderson, M. Schmidt, F. Schotte, P.A. Anfinrud, M. Wulff, K. Moffat, Visualizing reaction pathways in photoactive yellow protein from nanoseconds to seconds, Proc. Natl. Acad. Sci. U. S. A. 102 (2005) 7145–7150.

[18] C. Bernard, K. Houben, N.M. Derix, D. Marks, M.A. van der Horst, K.J. Hellingwerf, R. Boelens, R. Kaptein, N.A. van Nuland, The solution structure of a transient photoreceptor intermediate: Delta25 photoactive yellow protein, Structure 13 (2005) 953–962.

[19] E.C. Carroll, S.H. Song, M. Kumauchi, I.H. van Stokkum, A. Jailaubekov, W.D. Hoff, D.S. Larsen, Subpicosecond excited-state proton transfer preceding isomerization during the photorecovery of photoactive yellow protein, J. Phys. Chem. Lett. 1 (2010) 2793–2799.

[20] C.L. Perrin, J.B. Nielson, "Strong" hydrogen bonds in chemistry and biology, Annu. Rev. Phys. Chem. 48 (1997) 511–544.

[21] A. Warshel, A. Papazyan, P.A. Kollman, On low-barrier hydrogen bonds and enzyme catalysis, Science 269 (1995) 102–106.

[22] C.L. Perrin, Are short, low-barrier hydrogen bonds unusually strong? Acc. Chem. Res. 43 (2010) 1550–1557.

[23] S. Anderson, S. Crosson, K. Moffat, Short hydrogen bonds in photoactive yellow protein, Acta Crystallogr. D: Biol. Crystallogr. 60 (2004) 1008–1016.

[24] R. Brudler, T.E. Meyer, U.K. Genick, S. Devanathan, T.T. Woo, D.P. Millar, K. Gerwert, M.A. Cusanovich, G. Tollin, E.D. Getzoff, Coupling of hydrogen bonding to chromophore conformation and function in photoactive yellow protein, Biochemistry 39 (2000) 13478–13486.

[25] C.P. Joshi, H. Otto, D. Hoersch, T.E. Meyer, M.A. Cusanovich, M.P. Heyn, Strong hydrogen bond between glutamic acid 46 and chromophore leads to the intermediate spectral form and excited state proton transfer in the Y42F mutant of the photoreceptor photoactive yellow protein, Biochemistry 48 (2009) 9980–9993.

[26] A. Warshel, M. Levitt, Theoretical studies of enzymic reactions: dielectric, electrostatic and steric stabilization of the carbonium ion in the reaction of lysozyme, J. Mol. Biol. 103 (1976) 227–249.

[27] QSite, version 5.8, Schrödinger, LLC, New York, NY, 2012.

[28] K. Saito, H. Ishikita, Energetics of short hydrogen bonds in photoactive yellow protein, Proc. Natl. Acad. Sci. U. S. A. 109 (2012) 167–172.

[29] Y. Cao, M.D. Beachy, D.A. Braden, L. Morrill, M.N. Ringnalda, R.A. Friesner, Nuclear-magnetic-resonance shielding constants calculated by pseudospectral methods, J. Chem. Phys. 122 (2005) 224116.

[30] Jaguar, version 7.5, Schrödinger, LLC, New York, NY, 2008.

[31] A.K. Wolf, J. Glinnemann, L. Fink, E. Alig, M. Bolte, M.U. Schmidt, Predicted crystal structures of tetramethylsilane and tetramethylgermane and an experimental low-temperature structure of tetramethylsilane, Acta Crystallogr. B 66 (2010) 229–236.

[32] K. Saito, H. Ishikita, H atom positions and nuclear magnetic resonance chemical shifts of short H bonds in photoactive yellow protein, Biochemistry 51 (2012) 1171–1177.

[33] F. Hibbert, J. Emsley, Hydrogen bonding and chemical reactivity, Adv. Phys. Org. Chem. 26 (1990) 255–379.

[34] H.-H. Limbach, P.M. Tolstoy, N. Pérez-Hernández, J. Guo, I.G. Shenderovich, G.S. Denisov, OHO hydrogen bond geometries and NMR chemical shifts: from equilibrium structures to geometric H/D isotope effects, with applications for water, protonated water, and compressed ice, Isr. J. Chem. 49 (2009) 199–216.

[35] P.A. Sigala, M.A. Tsuchida, D. Herschlag, Hydrogen bond dynamics in the active site of photoactive yellow protein, Proc. Natl. Acad. Sci. U. S. A. 106 (2009) 9232–9237.

[36] K. Saito, H. Kandori, H. Ishikita, Factors that differentiate the H-bond strengths of water near the Schiff bases in bacteriorhodopsin and *Anabaena* sensory rhodopsin, J. Biol. Chem. (2012) 34009–34018.

[37] K. Saito, J.-R. Shen, T. Ishida, H. Ishikita, Short hydrogen-bond between redox-active tyrosine Y_Z and D1-His190 in the photosystem II crystal structure, Biochemistry 50 (2011) 9836–9844.

[38] M.E. van Brederode, T. Gensch, W.D. Hoff, K.J. Hellingwerf, S.E. Braslavsky, Photoinduced volume change and energy storage associated with the early transformations of the photoactive yellow protein from *Ectothiorhodospira halophila*, Biophys. J. 68 (1995) 1101–1109.

[39] H. Nymeyer, A.E. Garcia, J.N. Onuchic, Folding funnels and frustration in off-lattice minimalist protein landscapes, Proc. Natl. Acad. Sci. U. S. A. 95 (1998) 5921–5928.

[40] T. Matsui, T. Baba, K. Kamiya, Y. Shigeta, An accurate density functional theory based estimation of pK(a) values of polar residues combined with experimental data: from amino acids to minimal proteins, Phys. Chem. Chem. Phys. 14 (2012) 4181–4187.

[41] S. Hammes-Schiffer, Theoretical perspectives on proton-coupled electron transfer reactions, Acc. Chem. Res. 34 (2001) 273–281.